AD_____

AWARD NUMBER: W81XWH-08-1-0377

TITLE: Unraveling the Molecular Mechanism(s) Underlying ER+/PR- Breast Tumorigenesis Using a Novel Genetically Engineered Mouse Model

PRINCIPAL INVESTIGATOR: Hua Xiao

CONTRACTING ORGANIZATION: Michigan State University
East Lansing, MI 48824

REPORT DATE: September 2010

TYPE OF REPORT: Annual

PREPARED FOR: U.S. Army Medical Research and Materiel Command
Fort Detrick, Maryland 21702-5012

REPORT DOCUMENTATION PAGE

Form Approved
OMB No. 0704-0188

1. REPORT DATE *(DD-MM-YYYY)*	2. REPORT TYPE	3. DATES COVERED *(From - To)*
30-09-2010	Annual	1 SEP 2009 - 31 AUG 2010

4. TITLE AND SUBTITLE

Unraveling the molecular mechanism(s) underlying ER+/PR- breast tumorigenesis using a novel genetically-engineered mouse model

5a. CONTRACT NUMBER

5b. GRANT NUMBER
W81XWH-08-1-0377

5c. PROGRAM ELEMENT NUMBER

6. AUTHOR(S)
Hua Xiao

Email: XIAOH@msu.edu

5d. PROJECT NUMBER

5e. TASK NUMBER

5f. WORK UNIT NUMBER

7. PERFORMING ORGANIZATION NAME(S) AND ADDRESS(ES)

Michigan State University
East Lansing, MI 48824

8. PERFORMING ORGANIZATION REPORT NUMBER

9. SPONSORING / MONITORING AGENCY NAME(S) AND ADDRESS(ES)
U.S. Army Medical Research and Materiel Command

Fort Detrick, Maryland 21702-5012

10. SPONSOR/MONITOR'S ACRONYM(S)

11. SPONSOR/MONITOR'S REPORT NUMBER(S)

12. DISTRIBUTION / AVAILABILITY STATEMENT

Approved for public Release; Distribution unlimited

13. SUPPLEMENTARY NOTES

14. ABSTRACT Estrogen-receptor alpha (ERα)-positive Progesterone receptor negative (ER+/PR-) breast ductal carcinomas comprise approximately 15-25% of human breast cancers. However, molecular mechanisms underlying the development of this subtype of breast cancer remain poorly understood. This project is to study the molecular mechanism(s) underlying ER+/PR- breast tumorigenesis. Specifically, we proposed to determine genetic and epigenetic alterations in the initiation and progression of ER+/PR- mammary tumors arising in Tip30-/-/MMTV-neu mice. We previously demonstrated that *Tip30* deletion in MMTV-Neu mice significantly accelerates the formation of ER+/PR- mammary tumors. An unbiased DNA microarray analysis revealed that Tip30 deletion resulted in increased activation of cAMP-mediated signaling, EGF signaling, IGF signaling and PI3K/AKT signaling in ER+/PR- mammary tumors. Here we report that loss of Tip30 cooperates with Neu activation to enhance the activation of Akt signaling and ERα. Moreover, *Tip30* deletion led to delayed EGFR degradation and sustained EGFR signaling, and treatment of ER+/PR- mammary tumor cells with NVP-BEZ235 in combination with tamoxifen significantly inhibited cell proliferation compared to treatment with either NVP-BEZ235 or tamoxifen alone. Together, our data suggest NVP-BEZ235 in combination with tamoxifen as a potential therapeutic strategy for treating ER+/PR- breast cancers that are resistant to tamoxifen or trastuzumab.

15. SUBJECT TERMS
Estrogen receptor, Progesterone receptor, breast cancer, tumorigenesis

16. SECURITY CLASSIFICATION OF:			17. LIMITATION OF ABSTRACT	18. NUMBER OF PAGES	19a. NAME OF RESPONSIBLE PERSON
a. REPORT	b. ABSTRACT	c. THIS PAGE			USAMRMC
U	U	U	UU	17	19b. TELEPHONE NUMBER *(include area code)*

Table of Contents

Introduction:

It is estimated that 15-25% of all human breast cancers are ER+/PR- with more aggressive malignant characteristics and poorer response to SERMs compared to ER+/PR+ breast cancers (1-3). However, the molecular mechanism underlying development of ER+/PR- breast cancers still remains elusive (1). Our data indicates that deletion of *Tip30*, a tumor suppressor, leads to development of ER+/PR- in MMTV-Neu mouse model. The objective of this research project is to determine the molecular basis of ER+/PR- breast tumor development promoted by *Tip30* deletion. Our rationale for these studies is that elucidation of molecular basis of ER+/PR- breast tumor development has the potential to identify new therapeutic targets and strategies in the treatment, or even prevention, of breast cancers that are resistant to anti-estrogen therapy (2, 4). Specifically, we will determine genetic and epigenetic alterations in the initiation and progression of ER+/PR- mammary tumors arising in *Tip30*-/-/MMTV-Neu mice; and we will also evaluate IGF-I and Wisp-2 as potential therapeutic targets for ER+/PR- mammary tumors developed in *Tip30-/-* MMTV-Neu mice.

Body:

Task 1. **Determine specific genetic and epigenetic alterations in the initiation and progression of ER+/PR- mammary tumors arising in *Tip30*-/-/MMTV-Neu and *Tip30*+/-/MMTV-Neu mice.** The experiments proposed in Task 1a, b, and c were completed in year one. In response to the last review comments on the supporting data for gene expression, we report here that the genes are involved in ion and protein transportation, cell adhesion, cell proliferation and apoptosis signaling pathways (Appendix Table). Ingenuity pathway analysis of altered gene profiles revealed that cancer-associated pathways including EGF, IGF-I and PI3K/AKT signaling pathways were affected by *Tip30* deletion in Neu+ mammary tumors. These results indicate that besides increasing IGF-I signaling, enhancing other growth factor signaling pathways such as EGF signaling in mammary epithelial cells could also contribute to the development of ER+/PR- mammary tumors.

Deletion of *Tip30* leads to progressively increased numbers of p-Akt positive cells in the mammary glands from MMTV-Neu mice. The observation of increases in both EGF and IGF-I signaling pathways after deleting Tip30 led us to propose that PI3K/Akt and ERα are better targets for developing therapeutic strategies to inhibit ER+/PR- breast cancers. This is because both IGF-1 and EGF could activate PI3K/Akt, leading to phosphorylation of ERα and transcription activation of Wisp2 transcription. Therefore, it is not necessary to immediately analyze those differentially expressed signature genes and proteins as proposed in Task 1. In order to further demonstrate that the deletion of *Tip30* affects the activation of Akt (p-Akt), we first performed immunohistochemical analysis for p-Akt in preneoplastic mammary glands from *Neu+/Tip30*$^{-/-}$ and *Neu+/Tip30*$^{+/+}$ mice at the age of 2 and 12 months. MECs at the different ages exhibit negative, weak, intermediate or strong staining for p-Akt (Fig. 1; A1, A2, A3 or A4, respectively). No significant difference in p-Akt expression levels and numbers of p-Akt-positive cells (P = 0.678 or 0.972, respectively) was detected between *Neu+/Tip30*$^{-/-}$ and *Neu+/Tip30*$^{+/+}$ mammary glands at 2 months of age (Fig. 1B). However, at 12 months, the number of MECs having strongly positive p-Akt staining in *Neu+/Tip30*$^{-/-}$ mammary glands significantly increased compared to that in *Neu+/Tip30*$^{+/+}$ mammary glands (Strong staining in *Neu+/Tip30*$^{-/-}$ mammary gland: 41.4%; Strong staining in *Neu+/Tip30*$^{+/+}$ mammary gland: 9.9%; P = 0.02; Fig. 1C). There was no significant difference in the levels of p-Akt between mammary tumors from *Neu+/Tip30*$^{-/-}$ and *Neu+/Tip30*$^{+/+}$ mice (Fig. 1D). These data indicate that the relatively earlier onset of enhanced activation

p-Akt in the mammary glands due to *Tip30* loss may contribute to accelerated mammary tumorigenesis in *Neu+/Tip30*$^{-/-}$ mice.

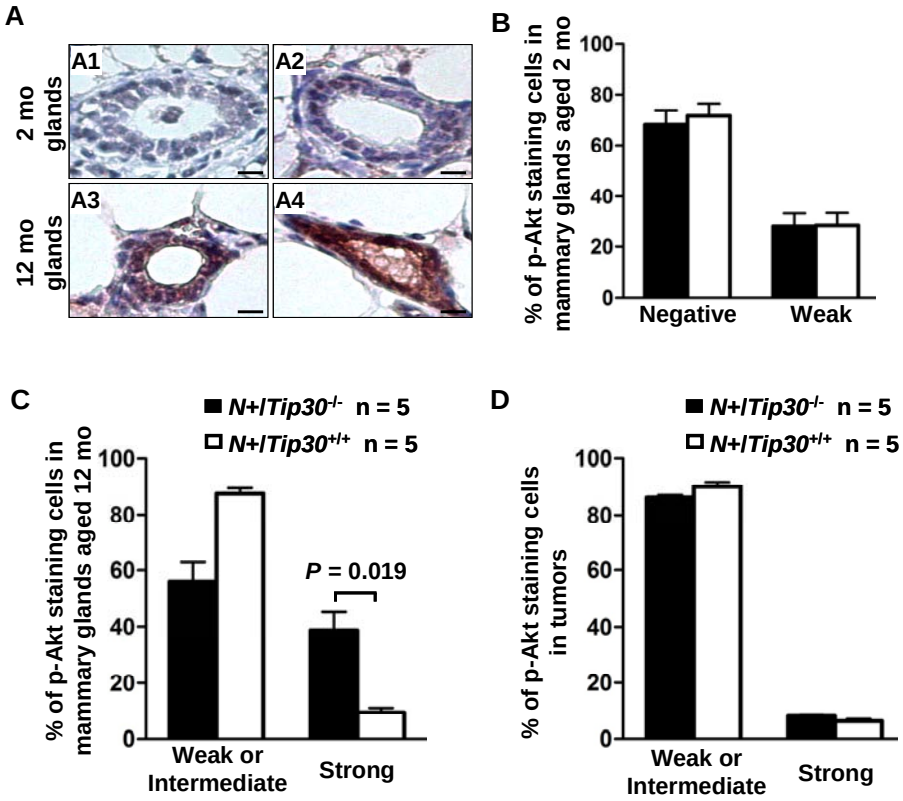

Fig.1. Representative immuno-histochemical staining for p-Akt in mammary tumors and mammary glands from *Neu+/Tip30*$^{-/-}$and *Neu+/Tip30*$^{+/+}$ mice. *A*, Representa-tive immunohistochemical staining of p-Akt in mammary glands. p-Akt staining in 2-month-old mammary glands ranges from negative to weak (A1 and A2) and is more intense in 12-month-old mammary glands (A3 and A4, intermediate and strong, respec-tively). Scale bar, 10 μm. *B-D*, Data represent means ± SEM of the percentage of cells that were stained positive or negative for p-Akt in 2-month-old (*B*) and 12-month-old (*C*) mammary glands and tumors (*D*) derived from *Neu+/Tip30*$^{-/-}$ and *Neu+/Tip30*$^{+/+}$ mice. Fifty cells were counted per field and 10 fields were counted per mouse. Data were analyzed by two-tailed *t* test.

Deletion of *Tip30* leads to a progressively increased numbers of p-ER positive cells in the mammary glands from MMTV-Neu mice. Given that ERα is activated through ligand binding and phosphorylation in response to estrogen and growth factor induced signaling and that *Tip30*$^{-/-}$ mice do not exhibit a significant increase in the number of ERα positive cells in the mammary glands at the age of 4 months (5), we therefore asked whether the proportion of p-ERα positive cells is altered in *Neu+/Tip30*$^{-/-}$ mammary glands. Immunohistochemistry analysis was used to examine phospho-ER (p-ERα) at Ser-171 (equivalent to Ser167 in human) in mammary glands and tumors from *Neu+/Tip30*$^{-/-}$ and *Neu+/Tip30*$^{+/+}$ mice (Fig. 2A). No significant difference in the numbers of p-ERα positive cells was detected in 2-month-old mammary glands from *Neu+/Tip30*$^{-/-}$ and *Neu+/Tip30*$^{+/+}$ mice (Fig. 2B). Strikingly, 12-month-old *Neu+/Tip30*$^{-/-}$ mammary glands and tumors displayed an increase in the number of p-ERα positive cells compared to *Neu+/Tip30*$^{+/+}$ mammary glands and tumors ($P < 0.05$). To test whether the *Tip30* gene promoter is active in ER+ epithelial cells and ER+/PR- tumors, we performed immunofluorescent double staining for ERα and β-galactosidase in the mammary glands and tumors derived from *Neu+/Tip30*$^{+/-}$ mice harboring a knock-in β-galactosidase (β-Gal) gene at the *Tip30* gene locus under the control of *Tip30* promoter. The β-Gal protein was predominantly detected in ER+ mammary epithelial cells and tumor cells (Fig. 2C), indicating that the *Tip30* promoter is activated mainly in ER+ MECs and tumor cells. Together, these results suggest that *Tip30* deletion preferentially increases the number of p-ERα positive luminal cells in the mammary gland of MMTV-Neu mice.

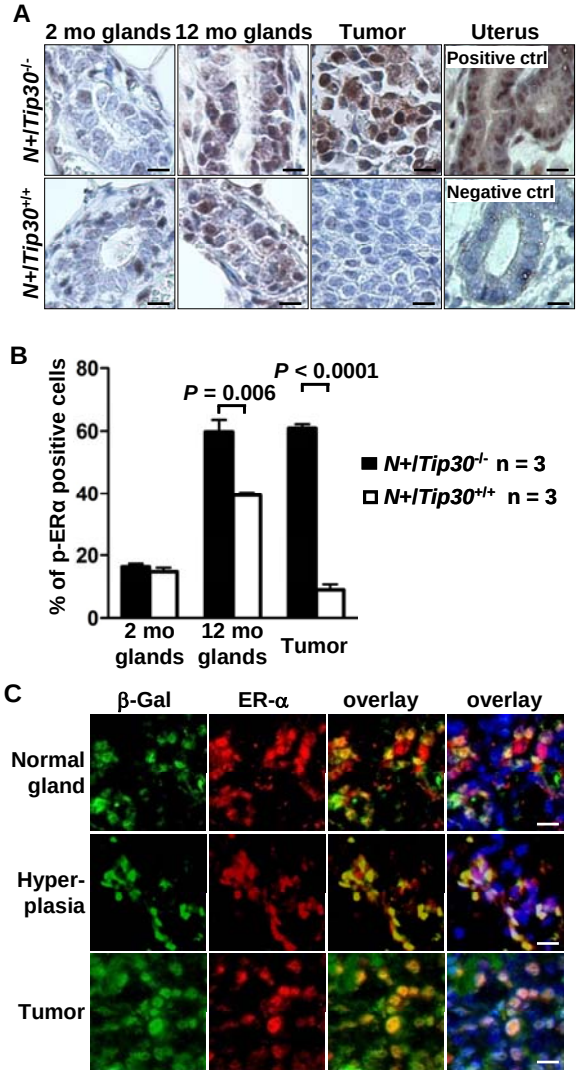

Fig. 2. Representative immunohistochemical staining of p-ERα in mammary glands and mammary tumors from *Neu+/Tip30*$^{-/-}$ and *Neu+/Tip30*$^{+/+}$ mice. *A*, Representative immunohistochemical staining of p-ERα in 2-month-old and 12-month-old mammary glands and mammary tumors from *Neu+/Tip30*$^{-/-}$ and *Neu+/Tip30*$^{+/+}$ mice. As a negative control, a uterus section was stained without using the primary antibody (anti-pERα). Scale bar, 10 μm. *B*, Data represent means ± SEM of the percentage of p-ERα positive cells in the mammary glands and tumors derived from *Neu+/Tip30*$^{-/-}$ and *Neu+/Tip30*$^{+/+}$ mice. p-ERα positive cells were counted in the sections of mammary glands and tumors derived from three mice of each genotype (randomly selected fields per section). 50 cells were counted per field and 10 fields were counted per mouse. *C*, Representative immunofluorescent double staining of mammary gland and tumor sections from a *Neu+/Tip30*$^{+/-}$ mouse for ERα (red) and β-Gal (green), following by counterstaining with DAPI (blue). Scale bar, 10 μm.

***Tip30* deletion leads to delayed EGFR degradation and sustained EGFR signaling.** Upon binding EGF, EGFR proteins are rapidly internalized and localized in early endosomes, where they are either sent back to the plasma membrane or sorted into late endosomes and lysosomes for destruction (6, 7). Early endosomes serve as a platform for signaling receptors to activate specific downstream signaling until ligand-receptor dissociation occurs due to early endosomal acidification mediated by vacuolar (H^+)-ATPases (8, 9). Recently, we have demonstrated that TIP30 regulates EGFR signaling by controlling endocytic downregulation of EGFR in primary hepatocytes and liver cancer cells. *Tip30* deletion impairs the fusion of Rab5 vesicles carrying vacuolar (H^+)-ATPases with early endosomes that contain internalized EGF and EGFR, leading to delayed EGFR degradation and sustained EGFR signaling (C. Zheng, L. Li and H. Xiao, submitted for publication). Therefore, we questioned whether the increased phosphorylation of Akt and ERα in *Neu+/Tip30*$^{-/-}$ mammary gland are also caused by a similar mechanism. First, we measured the protein levels of EGFR in mammary tumors cells isolated from *Neu+/Tip30*$^{-/-}$ and *Neu+/Tip30*$^{+/+}$ mammary tumors in response to EGF treatment at various times after EGF internalization. We used an experimental approach that eliminates the interference from continuous ligand internalization and nascent protein synthesis to measure endocytic degradation of EGFR. The comparison revealed that endocytic degradation of EGFR was significantly delayed in *Neu+/Tip30*$^{-/-}$ mammary tumors cells compared to *Neu+/Tip30*$^{+/+}$ mammary tumors cells, indicating that *Tip30* deletion impairs endocytic degradation of EGFR (Fig. 3A and B).

To determine whether *Tip30* deletion can block EGFR trafficking from early endosomes to lysosomes for degradation, we tracked Alexa-488 conjugated EGF (Alexa^{488}-EGF) and EGFR in normal primary MECs isolated from *Tip30*$^{-/-}$ and *Tip30*$^{+/+}$ mice. The majority of internalized EGF dissociated from EGFR in wild type MECs two hours after EGF internalization. In contrast, they remained associated with EGFR in

Tip30$^{-/-}$ MECs (EGF-EGFR colocalization in wild type primary MECs: 11%; EGF-EGFR colocalization in *Tip30*$^{-/-}$ primary MECs: 55%; n = 20, *P* = 0.004; Fig. 3C and D), indicating that *Tip30* deletion causes the trapping of EGF-EGFR complex in endosomes and sustained endosomal EGFR signaling. To rule out the possibility that *Tip30* deletion increased Neu transgene expression at the level of transcription, we used quantitative RT-PCR to examine the mRNA expression of Neu transgene in 5- to 9-week-old *Neu+/Tip30*$^{+/+}$ and *Neu+/Tip30*$^{-/-}$ mice and found no significant difference (data not shown). Together, these results suggest that Tip30 loss may prolong EGFR signaling, which cooperates with Neu activation to accelerate Akt activation and to promote the formation of ER+/PR- tumors.

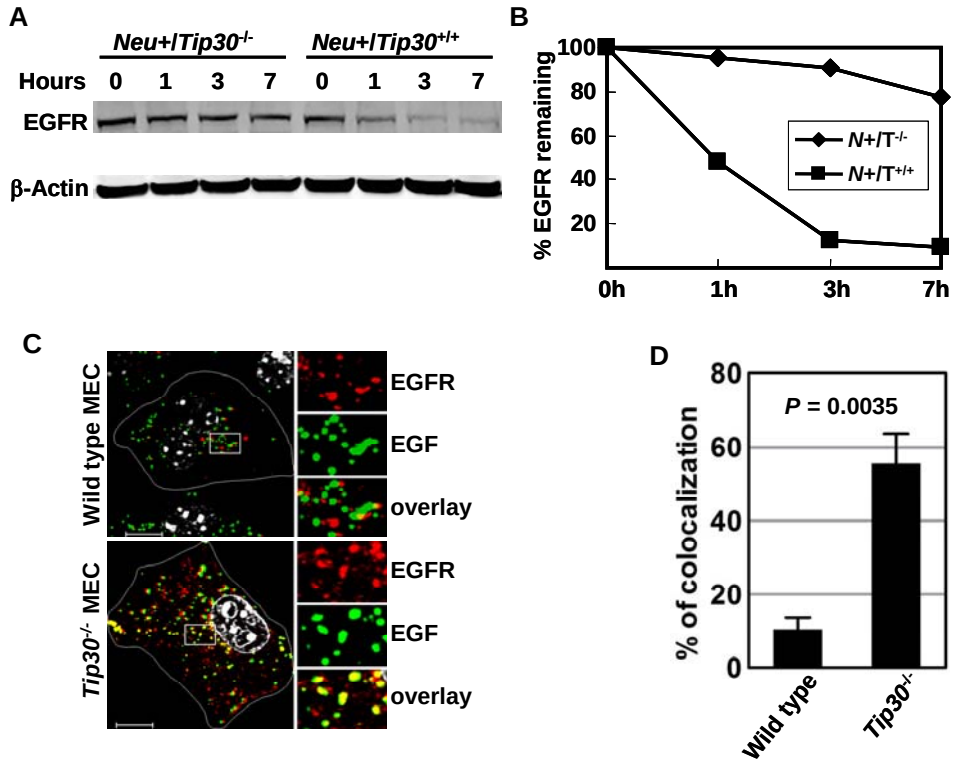

Fig. 3. Deletion of *Tip30* in MECs leads to delayed EGFR degradation. *A*, Mammary tumor cells isolated from *Neu+/Tip30*$^{-/-}$ and *Neu+/Tip30*$^{+/+}$ mice were incubated with 100 ng/ml of EGF for 1 hour on ice followed by washing with cold PBS and then incubated in serum-free medium containing 20 μg/ml of cycloheximide for the indicated times. Whole cell lysates were blotted with the indicated antibodies. *B*, Quantification of EGFR protein levels in (*A*) using Odyssey 2.1 software. *C*, Primary *Tip30*$^{+/+}$ and *Tip30*$^{-/-}$ MECs were subjected to EGFR internalization analysis. Representative confocal microscope images show the localization of EGFR (red) in endosomes after two hours of Alexa^{488}-EGF (green) internalization. Results are typical and representative of three experiments on primary cells from two mice of each genotype. Boxed areas are magnified. Representative cells are outlined in white. The colocalization of EGF and EGFR (yellow) in *Tip30*$^{-/-}$ cells is indicative of delayed endocytic degradation of EGFR; the nucleus was stained with DAPI (Grey). Scale bar, 10 μm. *D*, Quantitative analysis of EGF and EGFR colocalization. Twenty cells in each group were analyzed using MBF_imageJ. Pearson's colocalization coefficients were calculated and converted to percentages. *P* = 0.035; *t* test.

Task 2. Evaluate IGF-I and Wisp-2 as potential therapeutic targets for ER+/PR- mammary tumors developed in *Tip30-/-* MMTV-Neu mice. We have carried the experiments proposed in Task 2 in the second year. The preliminary findings led us to propose that PI3K is a better therapeutic for ER+/PR- mammary tumors.

AG1024, an IGF-IR inhibitor, can not effectively inhibit ER+/PR- mammary tumors developed in *Tip30*$^{-/-}$/MMTV-Neu mice. Our previous results showed IGF-1 and Wisp2 expression are increased in *Neu+/Tip30*$^{-/-}$ tumors; therefore, we have generated ER-/PR- and ER+/PR-*Tip30*$^{+/+}$/MMTV-Neu and

Tip30$^{-/-}$/MMTV-Neu mammary tumor cell lines for testing whether IGF-1 and Wisp2 (Task 2c) in year 2. The growth of ER+/PR- cells at the initial passages requires EGF and E2 (data not shown), but after cultured in vitro for 20 passages, the growth of these cells was independent of E2 (Figure 4. left panel). Based on our recent evidence that Tip30 loss also increases EGF signaling, we anticipate that inhibition of IGF-I and IGF-IR may not efficiently inhibit proliferation of ER+/PR- tumor cells. Indeed, addition of AG1024, an IGF-IR inhibitor, in the culture medium containing tamoxifen did not further affect proliferation of ER+/PR- mammary tumor cells derived from *Tip30-/-*/MMTV-Neu mice (Figure 4, right panel).

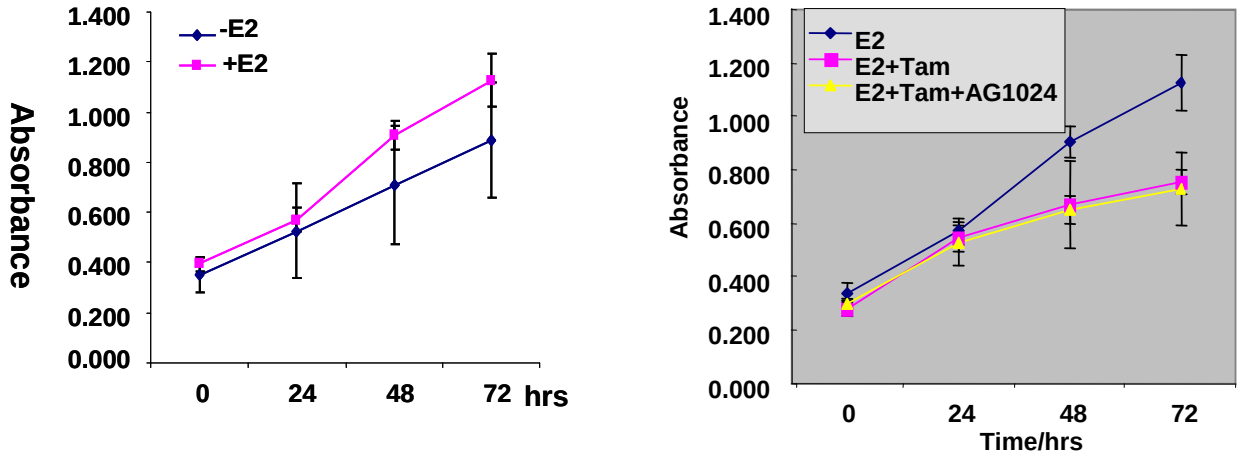

Fig. 4. Effect of AG1024 on the proliferation of ER+/PR- tumor cells. Cells were plated into 96-well culture plate in DMEM medium with 10% FBS. After 24 hrs, medium was replaced with phenol red-free DMEM supplemented with 10% charcoal-stripped FBS (Gibico). After starvation overnight, 10 nM E2 (left panel), or 10 nM E2, 1 uM tamoxifen plus nM E2, 1 uM tamoxifen plus nM E2 and 1uM AG1024 (right panel) were added to the indicated wells. Ethanol was used as vehicle control. Cell Counting Kit-8 (Dojindo, Japan) was used to measure cell proliferation at indicated times. Absorbance at 450 nm was measured using Fluostar Optima (BMG Labtech).

<u>Down-regulation of TIP30 results in resistance of tumor cells to trastuzumab.</u> To determine whether ER+/PR- tumor cells are sensitive to trastuzumab, we test the effect of trastuzumab on the proliferation of ER-/PR- and ER+/PR- tumor cell lines from Neu+/Tip30$^{+/+}$ mice or Neu+/TIP30$^{-/-}$ mice. As we predicted, ER+/PR- tumor cells were less sensitive to trastuzumab inhibition compared to ER-/PR- tumor

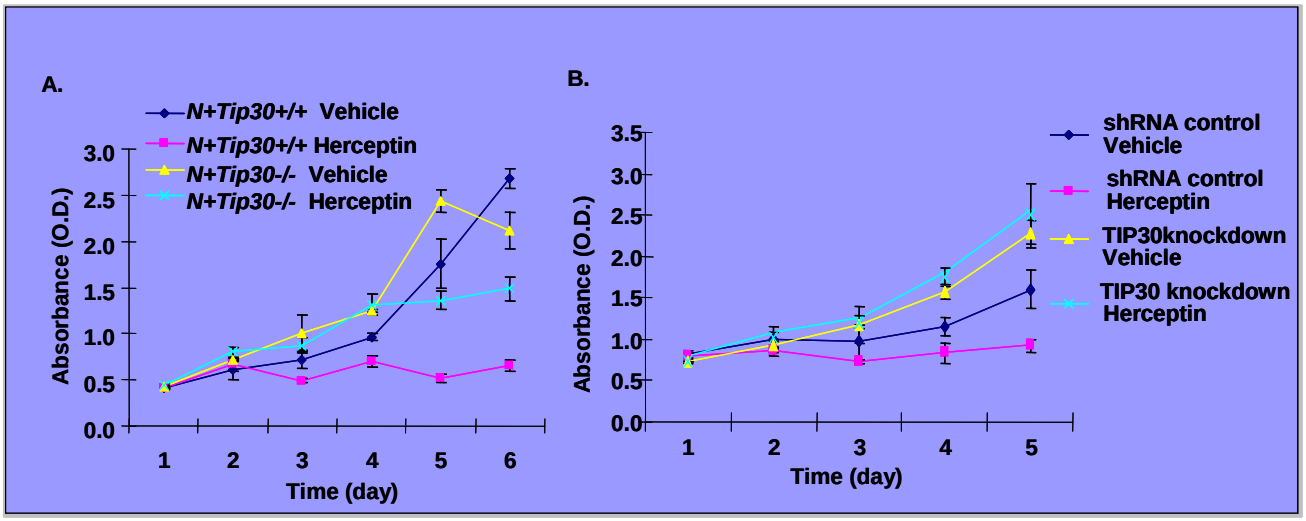

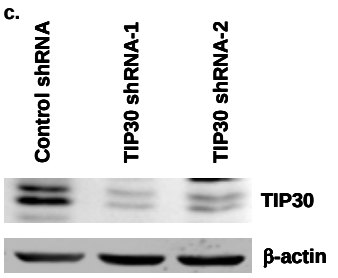

cells (Figure 5A). Similarly, knockdown of TIP30 in human HER2 positive breast cancer SKBr3 cells (HER2+/ER-/PR-) resulted in cells resistance to growth inhibition by trastuzumab (Figure 5B and C). These results suggest that TIP30 down-regulation leads to resistance of cancer cells to trastuzumab.

Fig. 5. Effect of trastuzumab on growth of breast cancer cells. ***A,*** Effect of trastuzumab on growth of mouse HER2+/ER+/PR- and HER2+/ER-/PR- tumors. Data are mean ± SE from three experiments. Statistical significance was analyzed by a t-test (*P < 0.01; HER2+/ER+/PR- cells versus HER2+/ER-/PR-cells). ***B,*** Effect of trastuzumab on growth of human breast cancer cells SKBr3 with or without TIP30 knockdown. The graph was generated from the experiments using control shRNA cells and TIP30-shRNA-1 SKBr3 cells. Data are mean ± SE from three experiments. Statistical significance was analyzed by t-test (*P < 0.01; TIP30 knockdown cells versus negative shRNA control cells). Tumor cells were seeded on day 0 in 96-well plates at 4×10^3 cells/well in DMEM, in the presence of saline or trastuzumab (50 μg/ml). Proliferation was analyzed using Cell Counting Kit-8 assay (Dojindo, Kumamoto, Japan) at indicated time points and absorbance at 485 nm was measured. The statistical significance was determined by using t test. ***C,*** Western blotting analysis of SKBr3 cells with control shRNA or TIP30-shRNAs. TIP30-shRNAs and control shRNA were purchased from Sigma-Aldrich Co. Preparation of shRNA lentiviruses and infection to SKBr3 cells was done according to manufacture's protocols.

<u>A combination of NVP-BEZ235 and tamaxifen has a better inhibitory effect on proliferation of ER+/PR- mammary tumor cells compared to the use of either NVP-BEZ235 or tamoxifen alone.</u>

Because the activation PI3K/Akt pathway is linked to multiple growth factors including IGF-I and EGF, PI3K would be an ideal candidate for combination therapies against ER+/PR- tumors. NVP-BEZ235 is a dual PI3K/mTOR inhibitor and effectively blocks phosphorylation of Akt and induces apoptosis of breast cancer cells having either HER2 amplification and/or PIK3CA mutation (10). Thus, we tested whether NVP-BEZ235 alone or in combination with tamoxifen affects proliferation of ER+/PR- tumor cells. Simultaneous treatment of ER+/PR- tumor cells with NVP-BEZ235 and tamoxifen robustly inhibits cell proliferation in vitro, whereas NVP-BEZ235 or tamoxifen alone treatment has only moderate or no inhibition of proliferation of the cells in vitro (Figure 6). These results suggest that a combined NVP-BEZ235 and tamoxifen treatment is a potentially effective strategy for treatment of ER+/PR- breast cancers.

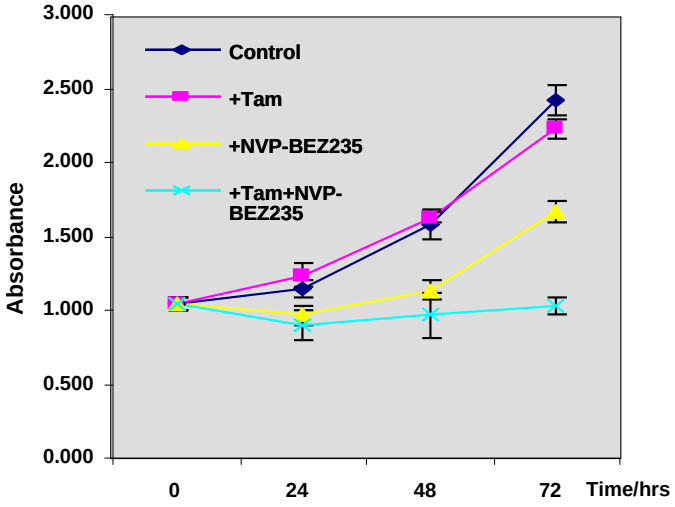

Fig. 6. Effect of NVP-BEZ235 and/or tamoxifen on growth of mouse ER+/PR- and HER2+/ER-/PR- tumors. Tumor cells were seeded in 96-well plates in DMEM, in the presence of DMSO, tamoxifen (1 μm), NVP-BEZ235 (250 nM) or tamoxifen (1 μm) plus NVP-BEZ235 (250 nM) at 0 hr. Proliferation was analyzed using Cell Counting Kit-8 assay (Dojindo, Kumamoto, Japan) at indicated time points and absorbance at 485 nm was measured. The statistical significance was determined by using t test.Data are mean ± SE from three experiments. Statistical significance was analyzed by a t-test (*P < 0.05; NVP-BEZ235 treatment versus control vehicle treatment; **P < 0.05; NVP-BEZ235 and tamoxifen treatment versus control vehicle treatment).

Key research Accomplishments:

1. Our data suggest that loss of Tip30 cooperates with Neu activation to enhance the activation of Akt signaling, leading to the development of ER+/PR- mammary tumors.

2. Our data demonstrate that *Tip30* deletion leads to delayed EGFR degradation and sustained EGFR signaling.

3. A combined NVP-BEZ235 and tamoxifen treatment has a better inhibitory effect on proliferation of ER+/PR- mammary tumor cells compared to the use of either NVP-BEZ235 or tamoxifen alone, implicating that combined inhibition of PI3K/Akt signaling and ERα as a therapeutic strategy against HER2+/ER+/PR- breast cancers that are resistant to tamoxifen or trastuzumab.

Reportable outcomes:

1. Part of this work is included in the manuscript entitled "*Tip30* Deletion in MMTV-Neu Mice Leads to Enhanced EGFR Signaling and Development of Estrogen Receptor-Positive and Progesterone Receptor-Negative Mammary Tumors ". The manuscript was reviewed by *Cancer Research* and requested for resubmission with responses to the comments by reviewers.

2. Part of this work is included in the PH.D. dissertation by Chengliang Zhang, a graduate student supported by this award, and his thesis has been defended successfully on Sept. 7, 2010.

3. A Breast Cancer DOD Idea award application entitled "Identification of a Novel Mechanism Underlying Resistance to HER2 Targeting Therapy" is submitted partly based on work supported by this award.

Conclusions: Our data suggest that enhanced EGFR signaling contributes to ER+/PR- breast cancers and a combined NVP-BEZ235 with tamoxifen treatment has a better inhibitory effect on proliferation of ER+/PR- mammary tumor cells compared to the use of either PI3K or tamoxifen alone.

References:

1. Arpino G, Weiss H, Lee AV, et al. Estrogen receptor-positive, progesterone receptor-negative breast cancer: association with growth factor receptor expression and tamoxifen resistance. J Natl Cancer Inst 2005;97:1254-1261.
2. Ponzone R, Montemurro F, Maggiorotto F, et al. Clinical outcome of adjuvant endocrine treatment according to PR and HER-2 status in early breast cancer. Ann Oncol 2006;17:1631-1636.
3. Kim HJ, Cui X, Hilsenbeck SGLee AV. Progesterone receptor loss correlates with human epidermal growth factor receptor 2 overexpression in estrogen receptor-positive breast cancer. Clin Cancer Res 2006;12:1013s-1018s.
4. Goss PE, Ingle JN, Martino S, et al. Efficacy of letrozole extended adjuvant therapy according to estrogen receptor and progesterone receptor status of the primary tumor: National Cancer Institute of Canada Clinical Trials Group MA.17. J Clin Oncol 2007;25:2006-2011.
5. Pecha J, Ankrapp D, Jiang C, et al. Deletion of Tip30 leads to rapid immortalization of murine mammary epithelial cells and ductal hyperplasia in the mammary gland. Oncogene 2007;26:7423-7431.

6. Hutchinson J, Jin J, Cardiff RD, Woodgett JR, Muller WJ. Activation of Akt (protein kinase B) in mammary epithelium provides a critical cell survival signal required for tumor progression. Mol Cell Biol 2001;21:2203-2212.
7. Allred DC, Brown P, Medina D. The origins of estrogen receptor alpha-positive and estrogen receptor alpha-negative human breast cancer. Breast Cancer Res 2004;6:240-245.
8. Forgac M. Vacuolar ATPases: rotary proton pumps in physiology and pathophysiology. Nat Rev Mol Cell Biol 2007;8:917-929.
9. Murphy JE, Padilla BE, Hasdemir B, Cottrell GSBunnett NW. Endosomes: a legitimate platform for the signaling train. Proc Natl Acad Sci U S A 2009;106:17615-17622.
10. Serra V, Markman B, Scaltriti M, et al. NVP-BEZ235, a dual PI3K/mTOR inhibitor, prevents PI3K signaling and inhibits the growth of cancer cells with activating PI3K mutations. Cancer Res 2008;68:8022-8030.

Upregulated genes

Gene symbol	Gene name	GenBank Accession#	Function	Fold change
Transport				
Rbp7	Retinoid binding protein 7	NM_022020	Transport	10.77
Slc38A1	Solute carrier family 38, member 1	NM_012038	Ion/amino acid Transport	9.04
Gabra4	Gamma-aminobutyric acid (GABA) A receptor, alpha 4	NM_010251	Transport	3.74
Gria4	Glutamate receptor ionotropic, AMPA 4	NM_019691	transport ion transport	3.00
Slc2a1	solute carrier family 2,member 1	NM_011400	transport	2.86
Scp2	Sterol carrier protein 2	NM_011327	lipid transport	2.40
Signal transduction				
Pik3cg	Phosphoinositide-3-kinase, catalytic, gamma polypeptide	NM_020272	Phosphorylation	2.73
Tacr3	Tachykinin receptor 3	NM_021382	G-protein coupled receptor protein signaling pathway	2.70
Mknk1	MAP kinase interacting serine/threonine kinase 1	NM_021461	protein kinase cascade	2.67
EGF	Epidermal growth factor	NM_010113	epidermal growth factor receptor signaling pathway	2.41
Arl4d	ADP-ribosylation factor-like 4D	NM_025404	small GTPase mediated signal transduction	2.30
Rab1b	Ras-related protein Rab-1B	NM_029576	small GTPase mediated signal transduction	2.30

Cell adhesion and cell cycle control				
Glycam1	Glycosylation-dependent cell adhesion molecule-1	NM_008134	Cell adhesion	8.02
G0s2	G0/G1 switch regulatory protein 2	NM_008059	cell cycle	5.27
Smoc1	Secreted modular calcium-binding protein 1	NM_022316	Cell adhesion	3.63
Crispld2	Cysteine-rich secretory protein LCCL domain containing 2	NM_030209	extracellular matrix organization	3.23
Spink5	Serine peptidase inhibitor, Kazal type 5	NM_001081180	regulation of cell adhesion/negative regulation of proteolysis	2.87
Cdkn1c	Cyclin-dependent kinase inhibitor 1C	NM_009876	cell cycle arrest	2.26
Casp6	Caspase 6, apoptosis-related cysteine peptidase	NM_009811	induction of apoptosis	2.13
Regulation of Transcription				
Cited4	CBP/p300-interacting transactivator 4	NM_019563	regulation of transcription	2.97
Barx2	BARX homeobox 2	NM_013800	regulation of transcription, DNA-dependent	2.46
Cdkn1c	Cyclin-dependent kinase inhibitor 1C (p57, Kip2)	NM_009876	negative regulation of transcription from RNA polymerase II promoter	2.25
Txnip	Thioredoxin interacting protein	NM_001009935	regulation of transcription, DNA-dependent	2.01
Protein degradation				
Lao1	L-amino acid oxidase 1	NM_133892	amino acid catabolic process	5.99

Ctsf	Cathepsin F	NM_019861	proteolysis	3.11
Spop	Speckle-type POZ protein	NM_025287	ubiquitin-dependent protein catabolic process	2.07
Rnf20	Ring finger protein 20	NM_182999	ubiquitin-dependent protein catabolic process // chromatin modification	2.03
Fbxo31	F-box protein 31	NM_133765	ubiquitin-dependent protein catabolic process	2.03

Downregulated genes

Gene symbol	Gene name	GenBank Accession#	Function	Fold change
Transport				
Apod	Apolipoprotein D	NM_007470	transport	16.38
Slc35f1	Solute carrier family 35, member F1	NM_178675	transport	4.78
Mup1	Major urinary protein 1	NM_031188	transport	3.69
Slc26a9	Solute carrier family 26, member 9	NM_177243	transport	3.19
Trpv6	Transient receptor potential cation channel, subfamily V, member 6	NM_022413	transport	3.15
Regulation of transcription				
Ifi205	Interferon activated gene 205	NM_172648	regulation of transcription, DNA-dependent	3.90
Ifi204	Interferon activated gene 204	NM_008329	regulation of transcription	3.63
Lass6	LAG1 homolog, ceramide synthase 6	NM_172856	regulation of transcription	2.90
Rbm39	RNA binding motif protein 39	AY061882	transcription	2.59
Signal transduction				
Serpina3f	serine (or cysteine) peptidase inhibitor	NM_001033335	response to cytokine stimulus	7.65

Il18r1	Interleukin 18 receptor 1	NM_008365	signal transduction	3.09
Rasgrp1	RAS guanyl releasing protein 1	NM_011246	intracellular signaling cascade	2.98
Angpt1	Angiopoietin 1	NM_009640	signal transduction	2.95
Gpr64	G protein-coupled receptor 64	NM_178712	signal transduction	2.77
Gprc5b	G protein-coupled receptor, family C, group 5, member B	NM_022420	signal transduction	2.65
Rassf9	Ras association (RalGDS/AF-6) domain family (N-terminal) member 9	NM_146240	signal transduction	2.55
Fgf13	Fibroblast growth factor 13	NM_010200	MAPKKK cascade	2.50
Vipr2	Vasoactive intestinal peptide receptor 2	NM_009511	G-protein coupled receptor protein signaling pathway	2.46
Gpr97	G protein-coupled receptor 97	NM_173036	G-protein coupled receptor protein signaling pathway	2.22
Cell adhesion and cycle control				
Htatip2	HIV-1 Tat interactive protein 2, 30kDa	NM_016865	cell cycle	5.37
Fmnl2	Formin homology 2 domain containing 2	NM_172409	cellular component organization	4.20
Vcan	Chondroitin sulfate proteoglycan	NM_001081249	cell adhesion	3.8
Protein degradation				

Cpe	carboxypeptidase E	NM_013494	proteolysis	6.52
St8sia6	ST8 alpha-N-acetyl-neuraminide alpha-2,8-sialyltransferase 6	NM_145838	protein amino acid glycosylation	5.83
Dpp10	Dipeptidyl peptidase IV-related protein 3	NM_199021	proteolysis	5.29
Rnf125	Ring finger protein 125	NM_026301	ubiquitin-dependent protein catabolic process	2.50
Ube2l6	Ubiquitin-conjugating enzyme E2L 6	NM_019949	ubiquitin-dependent protein catabolic process	2.33
Other biological process				
Tacstd2	Tumor-associated calcium signal transducer 2	NM_020047	biological_process	5.74
Adipoq	Adiponectin, C1Q and collagen domain containing	NM_009605	glucose metabolic process	5.62
Cxcl10	Chemokine (C-X-C motif) ligand 10	NM_021274	inflammatory response	3.75
Cyp2e1	Cytochrome P450, family 2, subfamily E, polypeptide 1	NM_021282	oxidation reduction	3.49